Video Article

Preparation of Murine Submandibular Salivary Gland for Upright Intravital Microscopy

Xenia Ficht*[1], Flavian Thelen*[1], Bettina Stolp*[1,2], Jens V. Stein[1]

[1]Theodor-Kocher Institute, University of Bern

[2]Center for Infectious Diseases, Integrative Virology, University Clinic of Heidelberg

*These authors contributed equally

Correspondence to: Jens V. Stein at jens.stein@tki.unibe.ch

URL: https://www.jove.com/video/57283
DOI: doi:10.3791/57283

Keywords: Immunology and Infection, Issue 135, Intravital imaging, mouse model, multiphoton microscopy, salivary gland, analysis of adaptive immune responses, immunology

Date Published: 5/7/2018

Citation: Ficht, X., Thelen, F., Stolp, B., Stein, J.V. Preparation of Murine Submandibular Salivary Gland for Upright Intravital Microscopy. *J. Vis. Exp.* (135), e57283, doi:10.3791/57283 (2018).

Abstract

The submandibular salivary gland (SMG) is one of the three major salivary glands, and is of interest for many different fields of biological research, including cell biology, oncology, dentistry, and immunology. The SMG is an exocrine gland comprised of secretory epithelial cells, myofibroblasts, endothelial cells, nerves, and extracellular matrix. Dynamic cellular processes in the rat and mouse SMG have previously been imaged, mostly using inverted multi-photon microscope systems. Here, we describe a straightforward protocol for the surgical preparation and stabilization of the murine SMG in anesthetized mice for *in vivo* imaging with upright multi-photon microscope systems. We present representative intravital image sets of endogenous and adoptively transferred fluorescent cells, including the labeling of blood vessels or salivary ducts and second harmonic generation to visualize fibrillar collagen. In sum, our protocol allows for surgical preparation of mouse salivary glands in upright microscopy systems, which are commonly used for intravital imaging in the field of immunology.

Video Link

The video component of this article can be found at https://www.jove.com/video/57283/

Introduction

Saliva is secreted by exocrine glands to lubricate food, protect the mucosal surfaces of the oral tract, and to deliver digestive enzymes as well as antimicrobial substances[1,2]. In addition to minor salivary glands interspersed in the oral submucosa, there are three bilateral sets of major glands identified as parotid, sublingual, and submandibular, according to their location[1,2]. Pyramid-shaped epithelial cells, organized into flask-shaped sacs (acini) or demilunes that are surrounded by myoepithelial cells and a basement membrane, secrete the serous and mucous components of saliva[1]. The narrow luminal space of the acini drains into intercalated ducts, which unite into striated ducts until they finally join into a single excretory duct[1]. The main excretory duct of the SMG is called Wharton's duct (WD) and opens into the sublingual caruncle[3,4]. The SMG epithelial compartment therefore represents a highly arborized structure with manifold terminal endpoints, resembling a bundle of grapes[1,5,6]. The SMG interstitium is composed of blood and lymphatic vessels embedded in connective tissue[7] containing parasympathetic nerves[8] and extracellular matrix[5]. Normal human and rodent salivary glands also contain T cells, macrophages, and dendritic cells[9], as well as plasma cells that secrete Immunoglobulin A (IgA) into the saliva[9,10]. Due to its multifaceted functions in health and disease, the SMG is a subject of interest for many fields of biological research, including dentistry[4], immunology[11], oncology[12], physiology[8], and cell biology[3].

Imaging of dynamic cellular processes and interactions is a powerful tool in biological research[13,14]. The development of deep tissue imaging and innovations inmicroscopes based on nonlinear optics (NLO), which rely on scattering or absorption of multiple photons by the sample, has allowed to directly examine cellular processes in complex tissues[13,15]. Absorption of multiple photons involves delivery of the total excitation energy by low energy photons, which confines fluorophore excitation to the focal plane and thus allows deeper tissue penetration with reduced photodamage and noise from out of focus excitation[13,15]. This principle is employed by two-photon microscopy (2PM) and allows for imaging of fluorescent specimens in depths of up to 1 mm[15,16]. While commercially available 2PM setups have become user-friendly and reliable, the major challenge for intravital imaging is to carefully expose and stabilize the target organ of anesthetized mice, especially for imaging of time lapse series. Several methods for digital drift correction after data acquisition have been published[17,18] and we recently developed "VivoFollow", an automated correction system, which counteracts slow tissue drift in real time using a computerized stage[19]. However, it is still critical for high quality imaging to minimize tissue motion, especially fast movements caused by breathing or heartbeat[19]. Preparation and stabilization procedures have been published for multiple organs, including spinal cord[20], liver[21], skin[22], lung[23], and lymph node[24]. Furthermore, models for rat salivary gland imaging have been developed[3,25] and further refined for high resolution intravital imaging of the murine SMG tailored to an inverted microscope setup[26,27,28].

Here, we present a practical and adaptable protocol for intravital imaging of the murine SMG using upright nonlinear microscopy, which is commonly used for intravital imaging in the field of immunology. To this end, we modified a widely employed immobilization stage used for popliteal lymph node preparations.

Protocol

All animal work has been approved by the Cantonal Committee for Animal Experimentation and conducted according to federal guidelines.

1. Anesthetize the Mouse

1. Wear personal protective equipment, including lab coat and gloves.
2. Mix ketamine, xylazine, and saline to a working concentration of 20 mg/mL and 1 mg/mL, respectively. Inject the working stock intraperitoneally (i.p.) at 8-10 µL/g of mouse. Place the mouse back into the cage.
   NOTE: This protocol has been tested for 6- to 40-week-old male and female mice with a C57BL/6 background.
3. Prepare the acepromazine solution at 2.5 mg/mL and inject 30 µL i.p., 15 min after the ketamine-xylazine injection (75 µg/mouse).
4. After 5-15 min, check for adequate anesthesia and analgesia by controlling for reflexes, *e.g.*, withdrawal reflex of the paw or corneal reflex.
5. Control for reflexes approximately every 30 min during the entire duration of the experiment. Subcutaneously inject ketamine/xylazine at 1.5 µL/g of mouse, every 60 min or earlier if reflexes are positive.
   NOTE: Inhalation anesthesia such as isoflurane cannot be used with this protocol, owing to the fixation of the mouse.

2. Remove the Fur from the Operating Area

1. Use an electric razor to shave an area that expands roughly from 5 mm caudal of the mouth towards the front legs, stretching over the jaws towards both ears.
2. Apply hair removal cream to the shaved area with a cotton swab. Carefully and thoroughly remove after 3 min, *e.g.*, by wiping with wet tissues.

3. Fix the Mouse on the Stage

NOTE: This protocol uses a customized stage (**Figure 1**) equipped with two freely adjustable holders for cover slips (one attached to the stage with a screw, the other fixed permanently onto it); adjustable stereotactic ear bars; a string, which can be tightened with a screw; a freely adjustable metal heating ring; and a raised area designated to place the torso of the mouse. This stage is modified from a popliteal lymph node stage, with an added stereotactic holder and a support for the lower cover slip holding the exteriorized SMG. Detailed plans or quotes of the stage are available upon request.

1. Prepare the stage by removing the holders for the heating ring and the removable cover slip holder. Loosen the screws of the ear bar holders and the fixed cover slip holder. Tape a piece of gauze to the center area of the stage, serving as bedding for the mouse.
2. Use glue (see **Table of Materials**) to attach a 20 mm diameter cover glass to the top of a cylindrical metal holder (this will be the lower cover glass). Glue a 25 mm cover glass to the bottom of the flat metal holder (this will be the upper cover glass). Ensure that the cover glasses overlap approximately 2-3 mm with metal holders and that the rest of the glass remains free of grease and glue.
3. Place the mouse on its back onto the gauze, perpendicular to the stretched string, with the head centered between the ear bars.
4. Fix the upper extremities of the mouse onto the stage with surgical tape.
5. Next, hook the string into the upper front incisors and tighten until the jaw reaches a horizontal position. Use an angled curved forceps to slightly pull out the tongue from the mouth, which facilitates breathing.
6. Tightly, but not forcefully, pull the tail and tape it to the stage.
7. Align the ear bars to achieve an angle of approximately 30° between the bar and the edge of the stage. To ensure this angle, use a triangle ruler to draw a right and left 30° angle on a sheet of paper, and place the transparent stage on the paper to align the holders accordingly.
8. Fix the jaw between the ear bars by simultaneously moving the left and right bar inwards until the jaw is immotile, and tighten screws. Observe chest movement before, during, and after fixing the jaw. Reduced or absent breathing indicates that the bars are fixed at the neck, not the jaw bone; in this case, repeat the fixing procedure immediately.
9. Provide heating to the mouse, *e.g.*, by placing a heating lamp nearby and/or a heating pad underneath the stage.

4. Surgical Exposure of the Salivary Gland Using a Stereomicroscope

NOTE: The following steps require the use of a stereomicroscope, fine forceps, and surgical scissors. Since the procedure is terminal, it is not necessary to maintain sterile operating conditions. Ethanol-cleaned instruments suffice.

1. Locate the approximate position of the right SMG lobe by looking for a slight bulge in the skin approximately 15 mm caudal of the mouth and 5 mm medial of the jaw line. Lift a small skin fold in the center of the bulge and cut it to create and opening of approximately 5 mm length.
2. Immediately apply a 4 mm-high ring of vacuum grease on the skin surrounding the cut. (Use a vacuum grease-filled syringe with a blunted 25 G hypodermic needle).
3. Fill the grease ring with saline to ensure the tissue remains moist during the operation.
4. Under the stereomicroscope, disrupt the connective tissue using the following procedure: Use one fine forceps to firmly hold a piece of connective tissue directly attached to the SMG, and use a second forceps to pull the distal connective tissue until it ruptures. Ensure that some connective tissue remains attached to the SMG; this is desirable since it allows handling. Do not touch the gland itself with the forceps, since this will cause bleeding.

5. Repeat this motion of disrupting connective tissue first on top of the gland, then on the medial side (between the right and left lobe of the SMG). Do not separate the sublingual from the submandibular gland.
6. Continue to remove the lateral connective tissue counterclockwise around the SMG (medial to caudal, to distal, to rostral).
7. Ensure that the blood supply, efferent lymphatics, and salivary duct, which are all located in a bundle at the cranial site of the gland, are not ruptured.
8. Once the lateral connective tissue is disrupted, use forceps to pull the connective tissue attached to the caudal end of the SMG upwards to lift the caudal end of the SMG. Disrupt the connective tissue below the SMG lobe, starting from the caudal and moving towards the rostral end.
9. Continue until the connective tissue to all sites of the SMG is removed (excluding the rostral site with major feeding/draining blood vessels and the WD).

5. Fixing the Gland

1. Confirm that the grease ring holding the saline is at least 4 mm high and not leaking (see step 4.2).
2. Install the lower cover glass (see step 3.2) by attaching the metal bar to its height-adjustable holder. Ensure that the cover slip holder is adjusted to the upmost position and does not touch the grease ring when attached to the stage. Position the holder from the caudal direction at an angle of approximately 60° to the mouse, with the cover slip covering roughly two thirds (caudal and distal parts) of the exposed lobe. Lower the cover glass until it makes contact with the gland.
3. Complete the grease ring on top of the cover glass to form a new saline reservoir.
4. Carefully pull the SMG lobe on top of the cover slip with forceps, only touching the connective tissue attached to it (the organ can be flipped with the bottom site facing upwards).
5. Ensure that the grease ring has an even height of at least 4 mm and does not leak. If necessary, refill the saline reservoir using a 30 G syringe filled with saline.
6. Ensure that the cover glass holder for the upper cover glass is in its upmost position. Use the screw to attach the metal holder with the 25 mm upper cover glass to the holder. Use the adjustable screws of the holder to position the cover glass so that the SMG is centered in the middle.
7. Use the screws of adjustable holder to lower the top cover glass until it directly contacts the SMG. Observe the shape and coloring of the gland during this step. If the gland surface area appears larger, or the coloring changes (for instance from pink to white), immediately put the cover glass to a higher position to relieve pressure on the SMG.
8. Check the saline reservoir for leaks by looking for air bubbles and or drops of saline outside the reservoir. If a leak or air bubble is detected, remove both cover slips and all grease and restart from step 2.
9. Screw shut all fixation screws.

6. Fixing the Heating Ring and Temperature Probe

1. Insert a temperature probe into the reservoir and position it close to the gland, then tape the probe wire to the stage.
2. Apply a grease ring to the top cover slip, with the SMG in the center (the diameter of the grease ring should correspond to diameter of the heating ring). Position the heating ring on top of the cover slip and seal with grease. Tape the tubing of the heating ring to the stage.

7. Imaging

NOTE: We use an upright two-photon microscope system equipped with a tunable Ti:Sa Laser and a fluorescent microscope with water-immersion 20X or 25X objectives. Real time correction of tissue drift during acquisition can be implemented by using an automated stage and VivoFollow[19]. This improves the stability of image acquisition, but is not required.

1. Turn on the upright microscopy system using an appropriate software provided by the microscope manufacturer. Tune the Ti:Sa Laser to a 780-900 nm excitation wavelength.
2. Connect the heating tubing to the heating ring. A peristaltic water pump circulates hot water (heated by submerging part of the tubing in an 80°C water bath) through the ring to warm the SMG.
3. Connect the temperature probe to a digital thermometer. Adjust the speed of the peristaltic pump if the temperature is not between 35-39 °C. The faster the pump works, the warmer the object gets, and vice versa.
4. Before starting image acquisition, perform a visual control of the blood flow velocities. Carefully check leukocyte passage through the thin capillaries or by fluorescent dextran injection.
   NOTE: Intravenously injected fluorescent dextran will immediately fill out the entire SMG vasculature when blood flow is physiological. This is virtually always the case in this procedure.
5. To follow immune cells, imaging depth is typically between 20-150 µm below the surface of the SMG identified by the 2nd harmonic generation signal. Record image stacks of 150-300 µm field of view with pixel resolution of approximately 512 x 512 or higher, and z-depths of 20-60 µm with spacing of 2-4 µm between images. Repeat stack acquisition every 20-30 s for a total duration of 20-60 min.
6. Use the digital thermometer to control the minimum and maximum temperature levels after acquisition of one image sequence. Discard the image sequence if the minimum or maximum are not in the range of 37 ± 2 °C. Refill the water for immersion of objective between image sequences.
7. At the end of the imaging session, euthanize the mice by CO_2 asphyxiation under anesthesia.
   NOTE: This is in accordance to Swiss federal guidelines of animal experimentation; other guidelines for euthanasia may apply elsewhere.

Representative Results

This protocol allows imaging of almost the entire dorsal or ventral side of the SMG. The field of view typically also includes the sublingual salivary gland, which differs slightly from the SMG in cellular composition[4]. Both glands are encapsulated by fibrillar collagen and subdivided into lobes. Most 2PM systems can produce a label-free image of fibrillar collagen by measuring the 2nd harmonic signal, but usually fluorescent molecules are needed for visualization of cellular and subcellular structures. For instance, ubiquitous transgenic expression of green fluorescent protein (GFP) in combination with the 2nd harmonic signal is sufficient to identify acini, ducts, and blood vessels in the SMG by their morphological features. This setup can be used to observe transgenic fluorescent markers with cell type specific expression to identify specific cell subsets. **Figure 2** shows a network ofCOL1A1-GFP reporter-expressing fibroblast-like cells of the connective tissue. Also shown are blood vessels, labeled by intravenous injection of a fluorescent dye coupled to high molecular weight dextran.The luminal compartment of the ducts can also be labeled (**Figure 3**) when the dye is injected retrogradually into the WD[29].

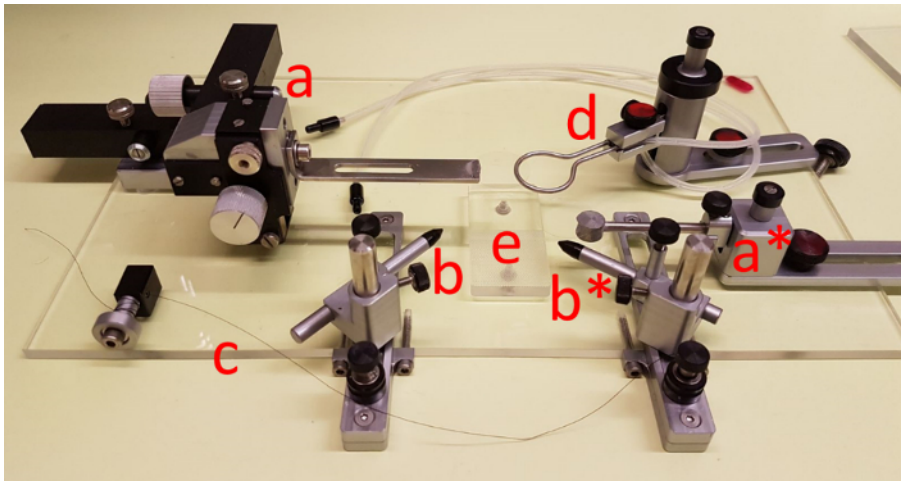

Figure 1: Customized stage. (a and a*) two freely adjustable holders for cover slips; (b and b*) adjustable stereotactic ear bars; (c) a string, which can be tightened with a screw; (d) a freely adjustable metal heating ring; (e) raised area designated to place the torso of the mouse. Please click here to view a larger version of this figure.

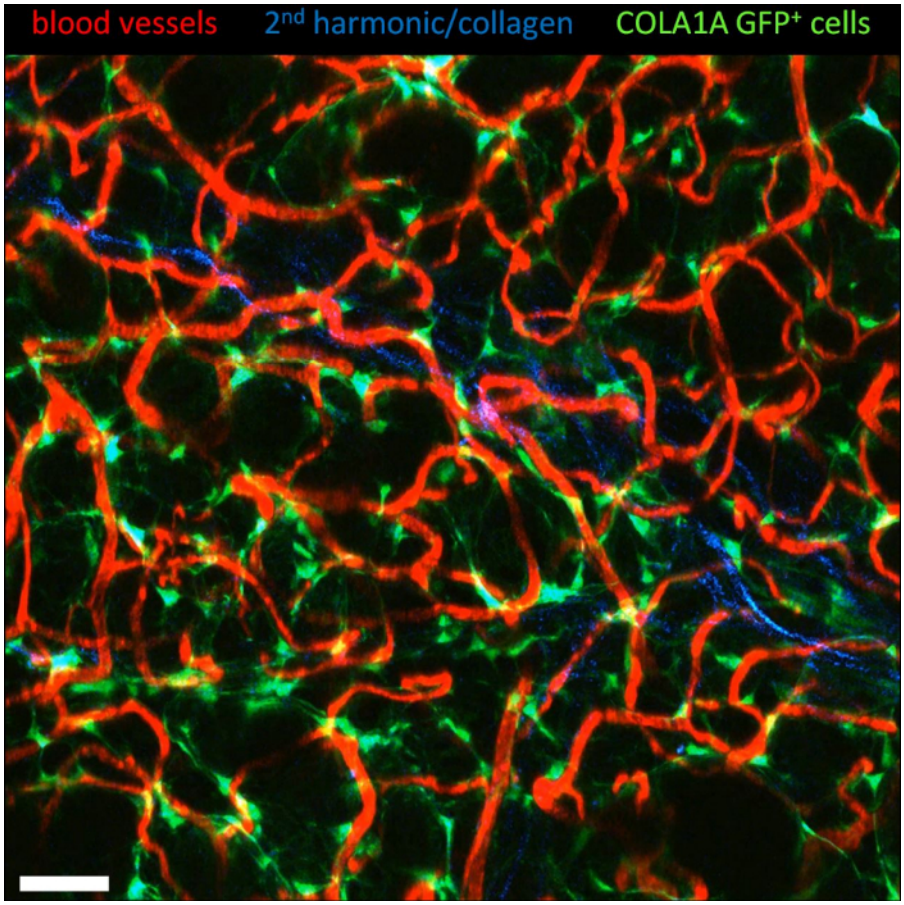

Figure 2: Vasculature marker (red) and network of COL1A1-GFP expressing cells (green). Vasculature labeled by intravenous injection of Texas Red-dextran conjugate (MW 70 kDa). Fibrillar collagen in between two lobes is visualized as the 2nd harmonic signal (blue). Shown is a single z-projection of 15 stacked images with 47 µm depth. Scale bar = 40 µm. Please click here to view a larger version of this figure.

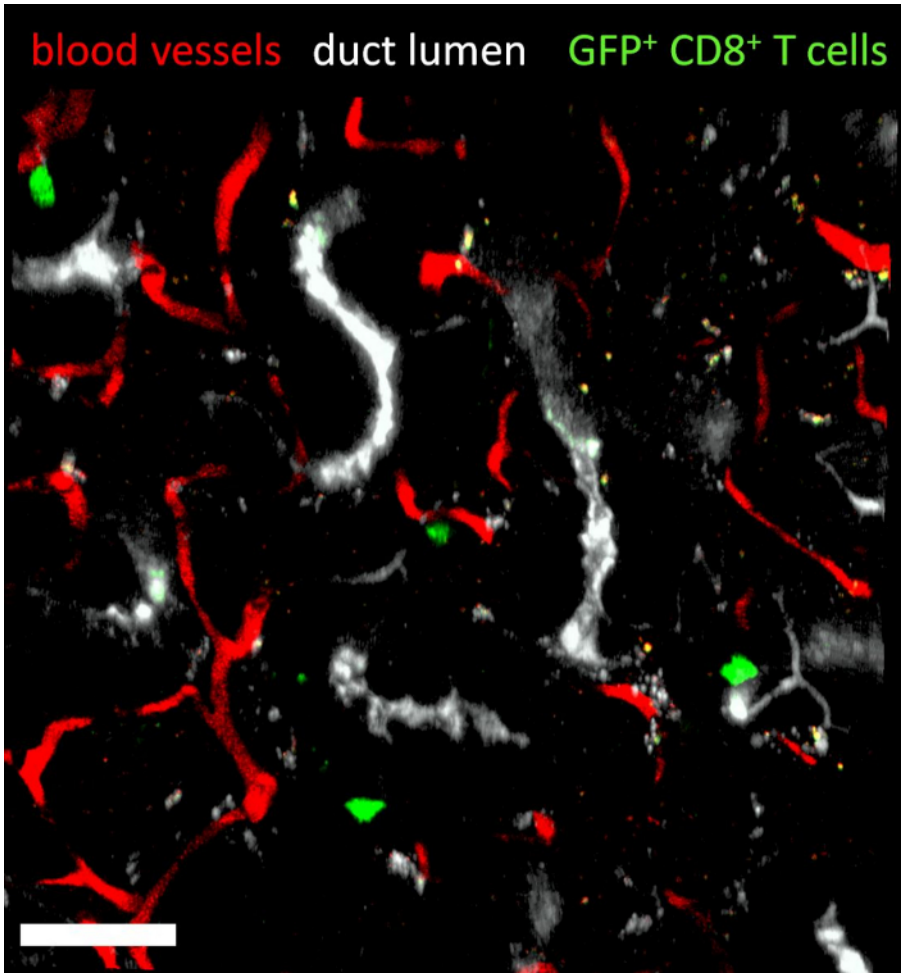

Figure 3: Luminal duct labeled after WD injection. Blood vessels labeled with 70 kDa-MW Texas Red-dextran (red), duct lumen labeled with cascade blue-dextran (white; 10 kDa MW) via retrograde injection through the WD and adoptively transferred GFP^+ $CD8^+$ T cells (green) in the SMG. Shown is a single z-projection of 27 stacked images with 50 µm depth. Scale bar = 40 µm. Please click here to view a larger version of this figure.

Discussion

This protocol offers a straightforward approach for *in vivo* imaging of murine submandibular and sublingual salivary glands using upright non-linear microscopy often used in the field of immunology. The method can be adapted for the imaging of other exocrine glands in the head and neck region. For instance, our lab has performed imaging of the lacrimal gland in an analogous manner (not shown).

Removing the connective tissue around the SMG is the most critical step of this protocol, since accidental tissue damage can occur. Damage to the main blood supply of the SMG necessitates immediate termination of the experiment, since the SMG tissue will become hypoxic. If the SMG tissue itself is damaged, bleeding typically stops naturally by coagulation. However, it needs to be considered that the injury triggers sterile inflammation and proinflammatory cytokines release[30], which could influence the experimental readout. A more common, but less critical complication during the microsurgery are leaks in the saline reservoir. To minimize the occurrence of leaks, always apply grease to dry, hairless skin. Patching a leak is usually futile: instead, remove all of the grease, clean the skin with a dry cotton swab, and reapply from scratch.

During imaging, a temperature close to the physiological body temperature must be maintained (approximately 37 °C for male and female C567BL/6 mice[31]). Since both hypo- and hyperthermia alter blood flow[32,33], physiological function of the SMG cannot be assumed under those conditions. However, we observed no difference in blood flow or T cell motility during small (± 2 °C), transient (<5 min) deviations from optimal temperature.

Minimizing tissue movement is essential for good imaging quality. Different kinds of unwanted tissue motion can occur, and have typical causes that can undergo troubleshooting. Firstly, continuous xyz-drift is usually caused by the SMG slowly drifting back into its original position through attached connective tissue. This happens if the lower cover glass was installed too high, or the connective tissue around the SMG was not thoroughly disrupted. Secondly, slow and continuous z-drift may occur if the temperature is unstable. In this case carefully adjust the heating and wait for the temperature to be stable, approximately 15 min before imaging. Finally, pulsating tissue motion occurs when the saline chamber is not tightly sealed. Pressure builds up and releases in the saline chamber with every breathing cycle. In combination with leaks or air bubbles this

leads to pulsating fluid flows, which translate directly to the SMG tissue. In this case, reassembly of both the cover glasses and saline chamber is the most reliable solution.

The maximum imaging depth depends on the excitation wavelength used and the fluorophores employed. As in virtually all intravital imaging setups, red-shifted dyes or fluorescent proteins that can be excited with long wavelengths (900-1,100 nm) allow for deeper tissue imaging than green dyes and shorter excitation wavelengths.

The SMG has been used as model organ for endo- and exocytosis and membrane remodeling[3,27,28], infection[34], autoimmunity[11], and tumor biology[12]. It further permits many forms of manipulation: dyes, pharmacological compounds, and antibodies can be delivered to the gland via the blood stream. Alternatively, the SMG can be targeted directly via the cannulation of the WD, which has been used to deliver virus[11], dextrans[3], DNA[25], dyes[29], or pharmacological agents[3].

The intravital imaging field continues to profit from an ever-growing toolbox of genetic and biochemical fluorescent labeling techniques. Advances in genetic engineering provide mouse lines and cell lines with sophisticated fluorescent markers. Recent examples include labeling of specific cell subsets ($CD11c^+$ cells[35]) or dynamic cytoskeletal proteins (Lifeact[36]), photoconvertible markers for cell tracking [37], and real-time reporters of nuclear translocation (NFAT[38]) or calcium signaling[39]. Other applications may use fluorescent biochemical probes, which highlight specific subcellular compartments (such as the DNA binding 4',6-diamidino-2-phenylindole (DAPI) or lipophilic membrane dyes). Modern NLO microscopy offers many possible solutions to best answer the experimental questions. For instance, multiplexed two-photon imaging has been developed to strongly increase maximum acquisition speed[40]. Other techniques offer label-free multiphoton imaging, either by generating second or third harmonic signals[15], or by measuring characteristic resonance vibration of molecules (coherent anti-Stokes Raman scattering)[41]. Thus, when practicable procedures for tissue exposure and stabilization are available, the limits of experimental design are mostly set by the experimenter's resources and creativity.

Disclosures

No conflicts of interest declared.

Acknowledgements

This work was funded by Swiss National Foundation (SNF) project grant 31003A_135649, 31003A_153457 and 31003A_172994 (to JVS), and Leopoldina fellowship LPDS 2011-16 (to BS). This work benefitted from optical setups of the "Microscopy Imaging Center" (MIC) of the University of Bern.

References

1. Pakurar, A.S., Bigbee, J.W. Digestive System. In: *Digital Histology.* Hoboken, NJ, USA: John Wiley & Sons, Inc.101-121 (2005).
2. Carpenter, G. Role of Saliva in the Oral Processing of Food. In: *Food Oral Processing.* Oxford, UK: Wiley-Blackwell 45-60 (2012).
3. Masedunskas, A., Weigert, R. Intravital two-photon microscopy for studying the uptake and trafficking of fluorescently conjugated molecules in live rodents. *Traffic.* 9 (10) 1801-1810 (2008).
4. Amano, O., Mizobe, K., Bando, Y., Sakiyama, K. Anatomy and histology of rodent and human major salivary glands. *Acta Histochem Cytochem.* 45 (5) 241-250 (2012).
5. Sequeira, S.J., Larsen, M., DeVine, T. Extracellular matrix and growth factors in salivary gland development. *Front Oral Biol.* 14 48-77 (2010).
6. Takeyama, A., Yoshikawa, Y., Ikeo, T., Morita, S., Hieda, Y. Expression patterns of CD66a and CD117 in the mouse submandibular gland. *Acta Histochem.* 117 (1) 76-82 (2015).
7. Hata, M., Ueki, T., Sato, A., Kojima, H., Sawa, Y. Expression of podoplanin in the mouse salivary glands. *Arch Oral Biol.* 53 (9) 835-841 (2008).
8. Proctor, G.B., Carpenter, G.H. Regulation of salivary gland function by autonomic nerves. *Auton Neurosci.* 133 (1) 3-18 (2007).
9. Le, A., Saverin, M., Hand, A.R. Distribution of Dendritic Cells in Normal Human Salivary Glands. *Acta Histochem Cytochem.* 44 (4) 165-173 (2011).
10. Hofmann, M., Pircher, H. E-cadherin promotes accumulation of a unique memory CD8 T-cell population in murine salivary glands. *Proc Natl Acad Sci.* 108 (40) 16741-16746 (2011).
11. Bombardieri, M., Barone, F., Lucchesi, D., et al. Inducible tertiary lymphoid structures, autoimmunity, and exocrine dysfunction in a novel model of salivary gland inflammation in C57BL/6 mice. *J Immunol.* 189 (7) 3767-3776 (2012).
12. Szwarc, M.M., Kommagani, R., Jacob, A.P., Dougall, W.C., Ittmann, M.M., Lydon, J.P. Aberrant activation of the RANK signaling receptor induces murine salivary gland tumors. *PLoS One.* 10 (6) e0128467 (2015).
13. Weigert, R., Sramkova, M., Parente, L., Amornphimoltham, P., Masedunskas, A. Intravital microscopy: A novel tool to study cell biology in living animals. *Histochem Cell Biol.* 133 (5) 481-491 (2010).
14. Masedunskas, A., Milberg, O., Porat-Shliom, N., et al. Intravital microscopy. *Bioarchitecture.* 2 (5) 143-157 (2012).
15. Zipfel, W.R., Williams, R.M., Webb, W.W. Nonlinear magic: Multiphoton microscopy in the biosciences. *Nat Biotechnol.* 21 (11) 1369-1377 (2003).
16. Theer, P., Hasan, M.T., Denk, W. Two-photon imaging to a depth of 1000 µm in living brains by use of a Ti:Al_2O_3 regenerative amplifier. *Opt Lett.* 28 (12) 1022 (2003).
17. Gomez-Conde, I., Caetano, S.S., Tadokoro, C.E., Olivieri, D.N. Stabilizing 3D in vivo intravital microscopy images with an iteratively refined soft-tissue model for immunology experiments. *Comput Biol Med.* 64 246-260 (2015).
18. Parslow, A., Cardona, A., Bryson-Richardson, R.J. Sample drift correction following 4D confocal time-lapse imaging. *J Vis Exp.* (86) (2014).
19. Vladymyrov, M., Abe, J., Moalli, F., Stein, J.V., Ariga, A. Real-time tissue offset correction system for intravital multiphoton microscopy. *J Immunol Methods.* 438 35-41 (2016).

20. Haghayegh Jahromi, N., Tardent, H., Enzmann, G., et al. A novel cervical spinal cord window preparation allows for two-photon imaging of T-Cell interactions with the cervical spinal cord microvasculature during experimental autoimmune encephalomyelitis. *Front Immunol.* 8 406 (2017).
21. Heymann, F., Niemietz, P.M., Peusquens, J., et al. Long term intravital multiphoton microscopy imaging of immune cells in healthy and diseased liver using CXCR6.Gfp reporter mice. *J Vis Exp.* (97) e52607 (2015).
22. Gaylo, A., Overstreet, M.G., Fowell, D.J. Imaging CD4 T cell interstitial migration in the inflamed dermis. *J Vis Exp.* (109) e53585 (2016).
23. Looney, M.R., Thornton, E.E., Sen, D., Lamm, W.J., Glenny, R.W., Krummel, M.F. Stabilized imaging of immune surveillance in the mouse lung. *Nat Methods.* (8) 91-96 (2011).
24. Liou, H.L.R., Myers, J.T., Barkauskas, D.S., Huang, A.Y. Intravital imaging of the mouse popliteal lymph node. *J Vis Exp.* (60) e3720 (2012).
25. Sramkova, M., Masedunskas, A., Parente, L., Molinolo, A., Weigert, R. Expression of plasmid DNA in the salivary gland epithelium: novel approaches to study dynamic cellular processes in live animals. *Am J Physiol Cell Physiol.* 297 (6) C1347-57 (2009).
26. Masedunskas, A., Porat-shliom, N., Tora, M., Milberg, O., Weigert, R. Intravital microscopy for imaging subcellular structures in live mice expressing fluorescent proteins. *J Vis Exp.* (79) e50558 (2013).
27. Masedunskas, A., Sramkova, M., Parente, L., et al. Role for the actomyosin complex in regulated exocytosis revealed by intravital microscopy. *Proc Natl Acad Sci.* 108 (33) 13552-13557 (2011).
28. Milberg, O., Shitara, A., Ebrahim, S., et al. Concerted actions of distinct nonmuscle myosin II isoforms drive intracellular membrane remodeling in live animals. *J Cell Biol.* 216 (7) 1925-1936 (2017).
29. Kuriki, Y., Liu, Y., Xia, D., et al. Cannulation of the mouse submandibular salivary gland via the Wharton's duct. *J Vis Exp.* (51) e3074 (2011).
30. Chen, G.Y., Nuñez, G. Sterile inflammation: Sensing and reacting to damage. *Nat Rev Immunol.* 10 (12) 826-837 (2010).
31. McLaren, A. Some causes of variation of body temperature in mice. *Q J Exp Physiol Cogn Med Sci.* 46 (1) 38-45 (1961).
32. Baumgart, K., Wagner, F., Gröger, M., et al. Cardiac and metabolic effects of hypothermia and inhaled hydrogen sulfide in anesthetized and ventilated mice. *Crit Care Med.* 38 (2) 588-595 (2010).
33. Crouch, A.C., Manders, A.B., Cao, A.A., Scheven, U.M., Greve, J.M. Cross-sectional area of the murine aorta linearly increases with increasing core body temperature. *Int J Hyperth.* 1-13 November (2017).
34. Smith, C.J., Caldeira-Dantas, S., Turula, H., Snyder, C.M. Murine CMV infection induces the continuous production of mucosal resident T cells. *Cell Rep.* 13 (6) 1137-1148 (2015).
35. Lindquist, R.L., Shakhar, G., Dudziak, D., et al. Visualizing dendritic cell networks in vivo. *Nat Immunol.* 5 (12) 1243-1250 (2004).
36. Riedl, J., Flynn, K.C., Raducanu, A., et al. Lifeact mice for studying F-actin dynamics. *Nat Methods.* 7 (3) 168-169 (2010).
37. Chtanova, T., Hampton, H.R., Waterhouse, L.A., et al. Real-time interactive two-photon photoconversion of recirculating lymphocytes for discontinuous cell tracking in live adult mice. *J Biophotonics.* 7 (6) 425-433 (2014).
38. Kyratsous, N.I., Bauer, I.J., Zhang, G., et al. Visualizing context-dependent calcium signaling in encephalitogenic T cells in vivo by two-photon microscopy. *Proc Natl Acad Sci U S A.* 114 (31) E6381-E6389 (2017).
39. Mank, M., Reiff, D.F., Heim, N., Friedrich, M.W., Borst, A., Griesbeck, O. A FRET-based calcium biosensor with fast signal kinetics and high fluorescence change. *Biophys J.* 90 (5) 1790-1796 (2006).
40. Tsyboulski, D., Orlova, N., Saggau, P. Amplitude modulation of femtosecond laser pulses in the megahertz range for frequency-multiplexed two-photon imaging. *Opt Express.* 25 (8) 9435 (2017).
41. Potma, E.O., Xie, X.S. Detection of single lipid bilayers with coherent anti-Stokes Raman scattering (CARS) microscopy. *J Raman Spectrosc.* 34 (9) 642-650 (2003).

